Performance of lightweight granulated glass concrete beams reinforced with basalt FRP bars

Gand, A., Sharif, S., Saidani, M., Lumor, R., Fom, P., Ogbologugo, U. & Yeboah, D.

Original citation:
Gand, A, Sharif, S, Saidani, M, Lumor, R, Fom, P, Yeboah, D & Ogbologugo, U 2019, 'Performance of lightweight granulated glass concrete beams reinforced with basalt FRP bars', Engineering Solid Mechanics, vol. Vol 7, no. 3, pp. 247-262.
https://dx.doi.org/10.5267/j.esm.2019.4.004

DOI 10.5267/j.esm.2019.4.004
ISSN 2291-8752
ESSN 2291-8744

Publisher: Growing Science

Engineering Solid Mechanics 7 (2019) 247-262

Contents lists available at GrowingScience

Engineering Solid Mechanics

homepage: www.GrowingScience.com/esm

Performance of lightweight granulated glass concrete beams reinforced with basalt FRP bars

Alfred Kofi Gand[a*], Shuaib Sharif[b], Messaoud Saidani[a], Richard Lumor[c], Pam Billy Fom[a], David Yeboah[d] and Ucheowaji Ogbologugo[a]

[a]*School of Energy, Construction and Environment, Coventry University, Coventry, UK*
[b]*Consultant Civil Engineer, UK*
[c]*School of Applied Sciences, Department of Civil Engineering, Central University College, Accra, Ghana*
[d]*Faculty of Engineering and Technology, Liverpool John Moores University, Liverpool, UK*

ARTICLE INFO

Article history:
Received 26 December, 2018
Accepted 18 April 2019
Available online
18 April 2019

Keywords:
Basalt
FRP
Rebars
Lightweight
Concrete
Granulated
Foam
Glass

ABSTRACT

This paper presents an investigation into the flexural behaviour of basalt FRP reinforced concrete beams through experimental and analytical methods. To achieve the research objectives, four concrete beams reinforced with steel and four identical concrete beams reinforced with BFRP bars were tested under four-point bending. The main parameters examined under the tests are the type of concrete (lightweight foam glass concrete and normal concrete) and the type of longitudinal reinforcement bars (BFRP and steel). Test results are presented in terms of failure modes; deformation crack pattern and the ultimate moment of resistance are presented. The experimental results are analysed and compared to predictive models proposed by ACI 440.1R, 2006 and BS EN 1992, Eurocode 2, for deformations and ultimate flexural capacities of the steel and BFRP reinforced concrete beams. The experimental results indicated that the flexural capacity decreased for the beams reinforced with BFRP bars compared to that of a corresponding beam reinforced with steel bars. Both types of beams failed in the modes predicted. The prediction models underestimated the flexural capacity of BFRP reinforced concrete beams. The increase in foam glass aggregate content was observed to reduce the cracking load by almost 10 - 40% and 25 - 50% for steel and BFRP reinforced concrete beams, respectively. The flexural capacities of BFRP reinforced beams were underestimated by using equations stipulated in ACI 440.1R and Eurocode 2 codes of practice.

1. Introduction

For more than a century, steel reinforced concrete structures have been constructed and used productively in all varieties of infrastructure works. As a result, their applications are at present governed by well-established design codes and ethical procedures. However, these standards are reviewed frequently to adapt to and reflect upon the latest findings and technological advancements. Sæther (2010) outlined that durability concerns and deterioration of reinforced concrete structures progress under aggressive exposure conditions. Corrosion of embedded steel reinforcement is a critical issue worldwide particularly for structures within proximity to coastal and marine environments. Internal corrosion of steel reinforcement in such aggressive environments can cause significant damage to reinforced concrete structures (in some severe cases even to structural failure) and also have considerable financial

* Corresponding author.
E-mail addresses: a.gand@coventry.ac.uk (A. K. Gand)

doi: 10.5267/j.esm.2019.4.004

repercussions requiring costly repair and maintenance operations. To overcome this issue, various measures and procedures have been developed and tested, yet none of these seemed to provide a practical and cost-effective solution. It was found that these remedies rather than permanently solve the corrosion problems; they were merely slowing down the process (Song & Saraswahty, 2007). In the last decade, the use of fibre reinforced polymer (FRP) bars as reinforcement material has emerged as a practical alternative solution (Barris et al*.,* 2012). FRP is a composite material made of continuous fibres consisting of high strength carbon, aramid or glass fibres embedded in a polymeric matrix (i.e. thermosetting resins) where the fibres primarily carry the load. Due to their inherent non-corrosive nature, utilisation of FRP reinforcement in new structures can increase service life and decrease maintenance and rehabilitation costs whereas in existing structures, the versatile nature of FRP, can allow retrofitting in an efficient manner which can provide significant savings in both construction costs as well as environmental benefits. FRP materials have a combination of physical and mechanical characteristics such as lightweight, high tensile strength, high stiffness, excellent durability and high fatigue strength.

Moreover, their non-corrosive, non-magnetic properties offer ideal solutions for external reinforcement and for applications where interferences with magnetic fields need to be avoided. Hollaway (2010) reported that at present, bridges, parking garages, highway infrastructure, marine environments, and chemical plants are sizeable examples of places where applications of FRP have been carried out fruitfully. Compared with conventional steel reinforcement, FRP rebars have a relatively low modulus of elasticity, low linear stress-strain behaviour until failure, and different bond properties, hence different structural response is expected. Nanni (2003) states that the design of FRP reinforced structures are often governed by the serviceability limit states (SLS), as the lower stiffness of FRP bars can lead to large strains under small loads resulting in large crack widths and deflections. Due to the variation of different mechanical and bond properties of FRP, that is primarily dependent on the category of fibre and manufacturing process; its design codes are not yet standardised. Although some studies have been focused on the investigation of the flexural behaviour of FRP reinforced concrete beams, there are insufficient experimental data and comparisons, particularly on lightweight and foam glass constituted elements. The use of granulated foam glass in concrete elements, particularly as beams and slab elements, provides a unique opportunity to reduce significantly, the permanent actions on superstructural and substructural elements. Whereas limited research has been done on concrete structural elements reinforced with conventional steel rebars, (Khatib et al., 2012), limited studies appear to exist for reinforced concrete beams utilising BFRP rebars.

Extensive research studies have been undertaken on steel reinforced concrete elements, beams in particular. Similar work has been carried or is ongoing for FRP reinforced and retrofitted concrete elements. Brik (2003) studied the bond strength between the modified basalt bars and compared the flexural capacity of the basalt reinforced concrete beams, by calculating the ultimate moment capacities in accordance with ACI 440.1R (2006). The investigation concluded that the bond between the modified basalt bars and the concrete was extremely good and that the ultimate experimental moment was much higher than the first cracking moment in all the tested beams. Also, the deformations were considerable indicating adequate ductility, with most of the beams, exhibiting principal flexural failures and that secondary shear failure was nominal. The study reinforced the potential of basalt FRP rebars as a suitable alternative for reinforced concrete structures.

By comparing existing standards such as the ACI 440.1R (2006), with studies done by Faza & GangaRao, (1993), Nanni (1993) and GangaRao & Vijay (1997), it can be demonstrated that the flexural capacity of concrete members reinforced with FRP bars can be determined using similar theoretical assumptions already established for steel reinforced concrete elements. Work undertaking by Alsayed et al. (2000) concluded that the flexural capacity of the beams reinforced by GFRP beams could be accurately predicted using the ultimate design theory.

According to West (2011), three possible modes of failure of the FRP reinforced beams exist, i.e. balanced failure, compression failure and tension failure. The modes of failure of concrete beam reinforced with FRP rebars greatly depend on the FRP reinforcement ratio compared to the reinforcement ratio achieved when the concrete crushes and FRP rupture simultaneously, i.e. a balanced reinforcement ratio. FRP reinforcement, when subjected to axial tension exhibits a linear elastic behaviour until failure. It is little, or no warning for these elements as the FRP elements would rupture before concrete crushing in compression for under reinforced beams, leading to the sudden and often catastrophic failure mode. For over-reinforced sections, the usual crushing of concrete would predominate, similar to steel reinforced sections. On the case of balanced sections, both the concrete and FRP rebar would achieve failure at the same time, albeit brittle in nature. Both modes of failures of FRP reinforced concrete beam are brittle due to the linear elastic behaviour of the FRP reinforcement bar. In 1993, Nanni (1993) stated that the concrete crushing failure mode is marginally more desirable for flexural members reinforced with FRP reinforcement bars. The ACI 440.1R standard (2006) recognises the two principal modes of failure for the design of flexural members reinforced with FRP bars, as far as strength and serviceability criteria are satisfied. Benmokrane et al. (1996) investigated the experimental and theoretical comparison between the flexural behaviour of concrete beams reinforced with glass FRP and steel counterpart by adopting the same analytical formulations put forward by Benmokrane et al. (1995) to determine the ultimate moment. Gao et al. (1998) undertook investigation focusing on the effects of reinforcement ratio on cracking patterns, deformation, flexural capacities, and modes of failure of GFRP and steel reinforced concrete beams. Theoretical correlations for the prediction of crack width, maximum deflection, and ultimate load carrying capacity were proposed based on the experimental investigation. When determining the ultimate flexural capacity of the beams, the researchers considered the effect of the compression reinforcement. Nevertheless, the effect was discounted as it was deemed negligible. From serviceability perspective, FRP and steel reinforced concrete elements behave differently. Deflection and crack width are normally relatively small compared to similar elements reinforced with FRP Bakis et al., (2002). The low elastic modulus of the FRP rebars results in large deflections and crack width compared to steel reinforcing bars (Kara & Ashour, 2012). Tests on basalt FRP reinforcement by Gohnert et al. (2014) concluded that four times the amount of basalt FRP was needed to achieve the same stiffness as that of the conventional steel reinforcements.

El Salakawy et al. (2002) states that at a service load limit, increasing the reinforcement ratio of the carbon FRP reinforced beams resulted in reduced deflections and tensile stresses in the carbon FRP reinforcements and subsequently, reduction in the crack width and propagation. Again, parallel results were achieved when different kinds of FRP composites were adopted. Designing FRP reinforced concrete beams for concrete crushing will significantly reduce deflections and crack width and thus to some extent satisfy serviceability criteria Nanni (1993). Understanding the bond characteristic of the FRP-concrete interface is important in understanding how the composite entity performs. Without sufficient bond between the FRP reinforcement and the concrete surround, the tensile strength and credentials FRP rebars are not fully optimised. Any form of slippage undermines the bond mechanisms. In this regard, several attempts objected at characterising the bond behaviour have been made. Cosenza et al. (1997) established that the bond characteristics vary from kind to kind of fibre reinforced polymers. Some composites exhibit higher bond strengths when compared to conventional steel whereas some FRP composites are associated with very low bond strengths. In the presence of adequate cover to prevent cracking, the bond strength of smooth, sand coated and helically threaded strands of FRP rebars was found not to be affected by concrete strength (Bakis et al., 2002). Mostofinejad and Moghaddas (2014) carried out several experiments to determine the effects of bar diameter on the FRP- concrete bond characteristics. Eight concrete beam specimens measuring 150 × 150 mm in cross-section and 350 mm long were subjected to a single shear load test of about 300 kN by use of a hydraulic jack. It was found out that the bond strength increased by 79% when bar diameters were doubled. A dissection of the basalt FRP reinforced concrete beam conducted by Gohnert et al., (2014) detected slippage at the end of the beams. This free end slippage of the beam can be incorporated in the bond strength design by allowing a value of 0.050 mm at the ends of beams as suggested by Wang & Belarbi (2005).

The shear performance of FRP reinforced concrete members has drawn attention from researchers. El-Sayed et al. (2006a) investigated the behaviour and shear strength of nine large-scale reinforced concrete slender beams, measuring 250 × 400 mm in cross-section and 3250 mm long and reinforced with FRP bars. The beams were tested in four-point bending. Test parameters were principally the reinforcement ratio and the modulus of elasticity of the longitudinal reinforcing bars. Three series of beams had three specimens each GFRP, CFRP, and steel reinforced. The study concluded that the low modulus of elasticity of FRP bars resulted in reduced shear strength compared to the shear strength of the reference steel reinforced beams. The study also concluded that ACI 440.1R (2003) prediction was conservative, particularly for beams reinforced with GFRP bars. Again, since the difference between the critical inclined cracking shear and the ultimate shear was small, El-Sayed et al. (2006a) and El-Sayed et al. (2006b) considered the cracking shear to be similar to the ultimate shear for all the test specimens, a consideration was in agreement with work undertaken by Tureyen & Frosch (2002).

Limbachiya et al. (2012) carried out a study on the effect of partially replacing fine natural aggregates and coarse natural aggregates with granulated foam glass (GFG) and reported that replacing the coarse natural aggregates with granulated foam glass would result in a significant strength loss and a reduction in the modulus of elasticity of the foam glass concrete whereas a gain in strength was recorded when fine natural aggregates were partially replaced with granulated foam glass. Their study revealed that, on the other hand, the flexural strength of the foam glass concrete would be slightly improved compared to normal weight concrete which is attributed to the more elastic nature of foam glass over natural aggregates contributing to an enhanced ductility and ultimate strength before failure. This agrees well with the results from the work of Kılıç et al. (2003), which show that lightweight concrete would gain a higher flexural tensile strength than normal weight concrete.

Jones & McCarthy (2005) carried out full-scale load-deformation tests on conventional lightweight foamed concrete beams to study the behaviour under flexural loading. Results from their study showed that lightweight reinforced concrete beam could sustain similar failure (flexural) loads as its counterpart normal weight concrete beam although having a higher value for deflection. The larger deflection of the reinforced foamed concrete beam is attributed to their lower modulus of elasticity. Further investigation into the failure modes for foamed concrete from their study showed that, just like its counterpart normal weight concrete, the foamed concrete displayed tensile cracks spread between the middle soffit of the beams with a few vertical cracks between the shear arm indicating a more brittle failure than normal weight concrete. However, Awang et al. (2015) outlined in their work that introducing fibres such as polypropylene into foamed concretes would improve their flexural strength even though it has less effect on the compressive strength; this is because of the resistance to bending stresses offered by the fibre resulting from inter-particle bond characteristics. Brady et al. (2001) in their review reported that fibres could also contribute to shear resistance in the foamed concrete. However, depending on the weight of the fibres and their concentration in the mix, they can also distort the structure of the foamed concrete (collapsing of foam) and settle to the bottom thereby weakening the material and causing irregularities. Some researchers have also investigated the influence of different additives such as fibers in crack initiation and propgation response of different concrete materials (Heidari-rarani et al. 2014; Fakhri et al. 2017; Rooholamini et al. 2018a,b; Aliha et al. 2012, 2017,2018; Razmi and Mirsayar 2017; Mansourian et al. 2018). Alnahhal and Aljidda (2018) investigated the flexural response of BFRP concrete beams using recycled concrete as the coarse aggregate constituent. The effect of the recycled coarse aggregate replacement ratio and the volume fraction of basalt micro-fibres were presented. The studies concluded that the ductility of the basalt FRP-concrete composite beams improved in comparison with those without basalt. Also, the effect of the recycled aggregate on the flexural capacities of the beams was insignificant and that the derived flexural capacities and deformations using code predictions reasonably agreed with the test results, particularly within the serviceability range. The foam glass in the foamed glass concrete mix could also improve the shear resistance, and flexural strength of lightweight concretes just like the polypropylene fibres. Replacing the steel reinforcement bars in these lightweight concrete beams with BFRP bars will further reduce the weight of the beams substantially and hence that of an entire structure.

From the preceding review, it is evident that although significant work has gone into understanding the behaviours of FRP reinforced concrete beams, little progress or no progress has been made when it comes to the coupled behaviour of lightweight concrete beams reinforced with basalt FRP composites, and hence the focus of this study.

2. Experimental programme

2.1 Constituents materials and mix proportions

For all concrete mixture combinations, the water-cement ratio and cement content were kept constant at 0.5, and 329 kg/m^3, respectively. The mixtures had proportions of 1 (cement): 2 (sand): 4 (coarse aggregate), with ordinary Portland cement used. The fine aggregates (sand) used were river sand with particle size distribution typically ranging from 63 μm to 4 mm. The coarse aggregates were gravel and stones with particles ranging from 4 mm to 20 mm in size. The foam glass (coarse aggregates) used as partial replacement of natural gravel were also similar in size, ranging from 4 mm to 20 mm. Its properties are presented in Table 1, with its physical representation shown in Fig. 1. Initial control mix consisted of natural coarse aggregates and the remaining mixtures were partially replaced with various amounts of lightweight foam glass aggregates in terms of volume. The percentage of foam glass content replaced was as follows: 0%, 10%, 20% and 30%. Table 2 presents details of the concrete mix combinations for the different series of beams. Presented in Table 3 are the experimental slump test values for different mix proportions. The results presented showed that generally, the partial replacement of natural coarse aggregates with foam glass content did not have significant impact on the slump values, and the fresh properties of the concrete mixes. The compressive strength of the tested cubes is presented in Table 4. The results show that the addition of foam glass aggregates yields a decrease in the compressive strength. Fig. 2 illustrates the development of compressive strength of foam glass concrete cubes over time, it is evident that in comparison to mix FG-0 (control mix); there is an early development of strength for the mixes containing foam glass aggregate replacement up to 14 days, after this period, the increase in strength is observed to be marginally insignificant. The results also indicate that a higher percentage of foam glass content results in a more substantial strength loss. For mix proportion FG10 with 10% foam glass content, the strength loss at 28-day age is approximately 8% whereas the strength loss in mix FG30 for the same age is almost 22%.

Fig. 1. Coarse foam glass aggregates

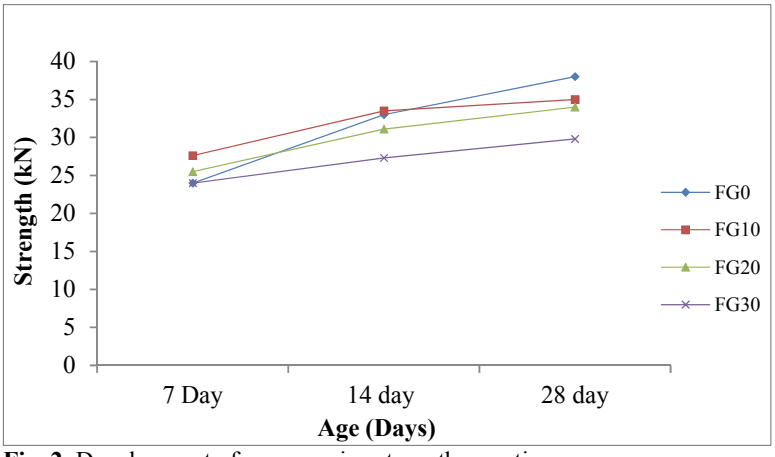

Fig. 2. Development of compressive strength over time

Table 1. Properties of foam glass aggregate.

Properties	Conventional coarse aggregate	Foam glass aggregate
Unit weight (g/cm^3)	1.50	0.55
Density (g/cm^3)	2.60	1.85
Water absorption capacity (%)	1.25	3.7
Percentage of voids	42	45

Table 2. Details of concrete mixes for the different series of beams

Material	FG0	FG10	FG20	FG30
Cement content (kg/m^3)	329	329	329	329
Water content (kg/m^3)	164.5	164.5	164.5	164.5
W/C ratio	0.5	0.5	0.5	0.5
Fine aggregate – river sand (kg/m^3)	657.96	657.96	657.96	657.96
Coarse aggregate – natural gravel (kg/m^3)	1315	1183.5	1052	920.5
Coarse aggregate – foam glass (kg/m^3)	-	18.69	37.38	56.07

Table 3. Mix proportion and experimental values for slump test.

Mix code	Percentage foam glass replacement	water/cement ratio	slump value ($\pm$ 10mm) (mm)
FG0	0%	0.5	70
FG10	10%	0.5	65
FG20	20%	0.5	60
FG30	30%	0.5	50

Table 4. The compressive strength of foam glass concrete

Mix code	Foam glass content	Compressive strength (MPa) (Days)			Difference in strength (%)		
	(%)	7	14	28	7	14	28
FG0	0	24.0	33.0	38.0	0	0	0
FG10	10	27.6	33.5	35	+15	+1.5	-7.9
FG20	20	25.5	31.1	34.0	+6.3	-5.8	-10.5
FG30	30	23.5	27.3	29.8	-2.1	-17.3	-21.6

2.2 Reinforcing bars

Basalt fibre reinforced polymer (BFRP) rods, also referred to as rockbars, is low weight, economical, high tensile, corrosion resistant and non-conducting inorganic fibre material. It is pultruded from naturally occurring volcanic basalt rock deposits in a single melt process. The BFRP used in the experimental research was 10 mm diameter reinforcement rods with a coarse-grain sanded finish for improved bonding which was manufactured and supplied by MagmaTech Ltd., UK. The BFRPs polymer matrix consisted of continuous basalt fibre filaments and epoxy resin, which comprises both mechanical characteristics of the synergistic materials. Basalt as a composite material was used for the tests due to its exceptional corrosive and heat resistance properties, which have gained interest for its benefits in the replacement of asbestos fibres in the construction sector. It is also significantly lighter than conventional steel while exhibiting a higher tensile strength. Table 5 defines the experimentally determined material specification of the basalt FRP and steel rebars used in the study.

Table 5. Properties of BFRP and steel reinforcement

Type of bar	Diameter (mm)	Ultimate tensile strength (MPa)	Ultimate strain	Elastic Modulus (GPa)
Steel (SL)	10	545	Not measured	200
BFRP (BF)	10	675	Not measured	336

2.3 Test programme

To evaluate the relative flexural behaviour of the beams, four mixes were considered for the production of eight rectangular reinforced concrete beam test specimens. Each mix comprised two beams, one containing BFRP rebar and the other reinforced with conventional steel reinforcement for comparison purposes. The beams were divided into series designated as S-x and B-x. The first term identifies the series of the beams whereas the second term corresponds to the concrete mix. For example,

beam series S-10 denotes steel reinforced beam containing 10% granulated foam glass replacing natural gravel. The total length of each beam was 1500 mm. The cross-sections measured 85 mm wide and 185 mm depth as shown in Table 6. All beams were tested under a quasi-static four-point bending method as illustrated in Figs. 3 and 4. To measure the deflection, linear variable differential transformers were placed at mid-span. The loading apparatus consisted of a spreader beam supported by 60 mm circular rollers. Pinned and roller support conditions were provided, as illustrated. The load was applied vertically downward by load control, by means of a Denison test machine with a capacity of 500 kN, and controlled hydraulically. Strain distribution was measured using demec points affixed to the concrete surface. The failure mechanisms of the beams during testing were monitored and recorded for analysis. The load was applied in 3 kN increments until failure, after every load interval the strains were manually recorded using a digital mechanical strain gauge.

Table 6. Geometric characteristics of all the specimens

Series	Cross-section dimensions width × depth (mm)	Beam effective span (mm)	Main reinforcement	Shear links size/spacing
BFRP	85 × 185	1200	2no - 10Ø	H8-90
Steel	85 × 185	1200	2no - 10Ø	H8-90

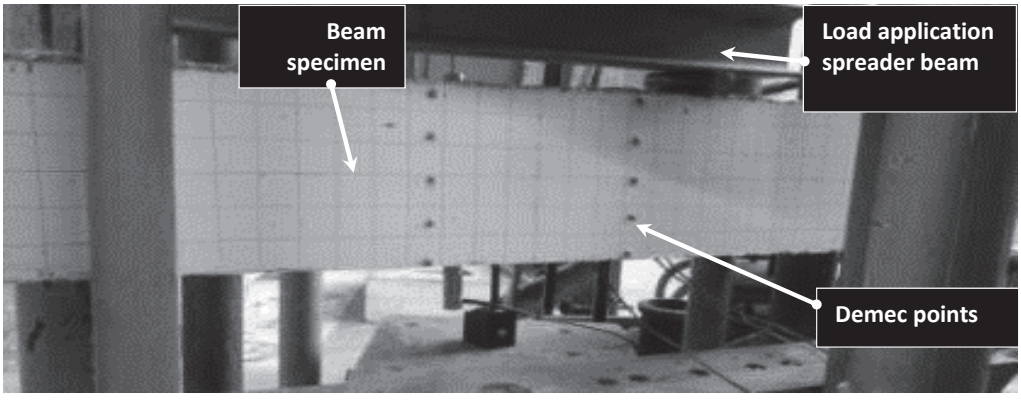

Fig. 3. Typical experimental set-up.

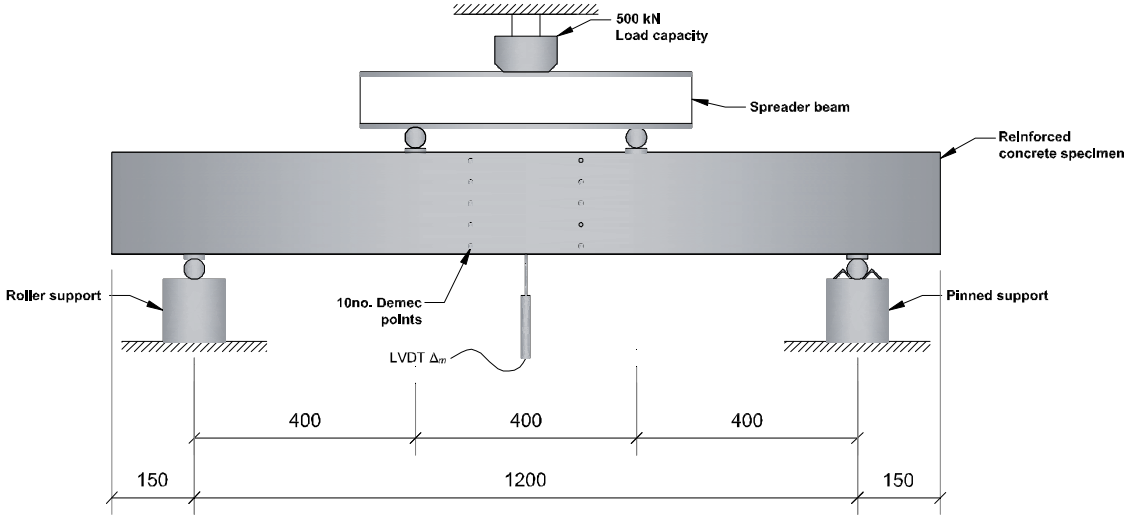

Fig. 4. Schematic test arrangements.

3. Results and discussion

3.1 Cracking and mode of failure of steel reinforced beam specimens

The steel reinforced concrete beams consisted of 2no. 8 mm diameter high tensile steel rebars as main tension reinforcement. The first vertical flexural crack in the beams occurred at a relatively small load of between 20 - 35%, i.e. 15 – 21 kN of their ultimate load, in the constant bending moment region. With further load increase, additional flexural cracks developed along the span of the beam length. The cracks propagated outside the flexural zone and started to take a diagonal shape towards the compression fibres of the beam. However, the width of these flexural cracks did not change significantly, suggesting that they were all secondary flexural cracks. Secondary cracks are those that are widely spaced and occur under low loads without influencing other cracks to arise. These cracks develop during the initial stages of the cracking due to internal expansion and contraction of the concrete constituents as well as low flexural stresses accumulating from the self-weight of the beam. Hassoun and Al-Manaseer (2008) stated that, when steel bars are subjected to low tensile stresses, the widths of the cracks remain small, but the numbers of cracks increase. As the tensile stresses progress further, an equilibrium stage is reached. When the tensile stresses are further increased to a point, that between the steel and the concrete there is a difference in strain, then the second stage of the cracking starts to occur, where the widths of the cracks increase without any significant increase in the number of cracks. These cracks are known as the main cracks. Usually, one or two cracks start to widen more than the others, forming critical cracks. This was observed during the experiment from 36 – 45 kN loads for the specimens until failure. The cracks started to widen and extend towards the top compression fibres of the beams without any additional cracks forming. The beams continued to sustain loads to reach the highest flexural capacity, at which the concrete in the compression region was crushed. The steel reinforced beams exhibited flexural failure by yielding of the steel reinforcement followed by concrete crushing in the compression zone, typically outlined in Fig. 5. The concrete crushing for all of the steel reinforced beams initiated within proximity to the top middle zone of the beam by widening of the vertical cracks. Moreover, it was observed that the width of a major crack increased faster than the neighbouring cracks. As the applied increased, concrete at the top compression zone started to spall and a subsequent progressive failure occurring. Although failure by concrete crushing is brittle, some ductility was observed in all the steel reinforced beams. This is attributed to the plasticity of the concrete in compression before reaching its final stage. The prolonged deflection of beam reference SL - 0 at near maximum load, provided ample warning before failure thus indicating ductility behaviour.

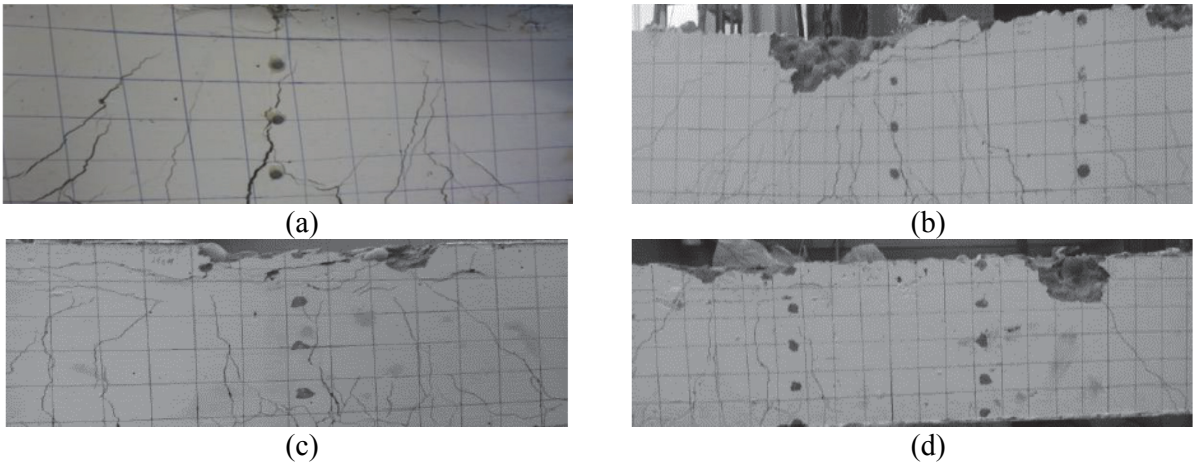

Fig. 5. Failure pattern of steel RC beams (a) SL-0; (b) SL-10; (c) SL-20; (d) SL-30

3.2 Load-deflection response of steel reinforced beam specimens

The load-deflection relationships for the steel reinforced concrete beams are shown in Fig. 6. It is evident that generally, in all the beams, the load-deflection plots during the un-cracked elastic stage

represented by the first slope is steep and linear up to the first flexural crack. The deflection when the first cracks appeared at approximately 15 - 21 kN was recorded to be 0.64 - 1.26 mm. Once these flexural cracks were formed, a slight change in the slope of the load-deflection curve was observed, and this remained linear until yielding of the steel reinforcement took place, represented by the second stage of the slope. As the load increased, the deflections also increased. However, it was observed that the beams with higher foam glass content deflected less under smaller loads in comparison to beams with lower foam glass content, i.e. beam SL - 20 deflected less than SL - 0 under smaller loads. For example, at 12 kN, the deflection for beam SL - 20 was recorded to be 0.35 mm whereas beam SL - 0 had a deflection of 0.85 mm. This shows that the stiffness of the beam is increased and the deflection is decreased when the foam glass content is increased. With further load increase beyond the yielding of the tensile steel reinforcement, all the load-deflection curves enter into the plastic region and show a drastic change in the slope which is almost horizontal up to the ultimate failure of the beams.

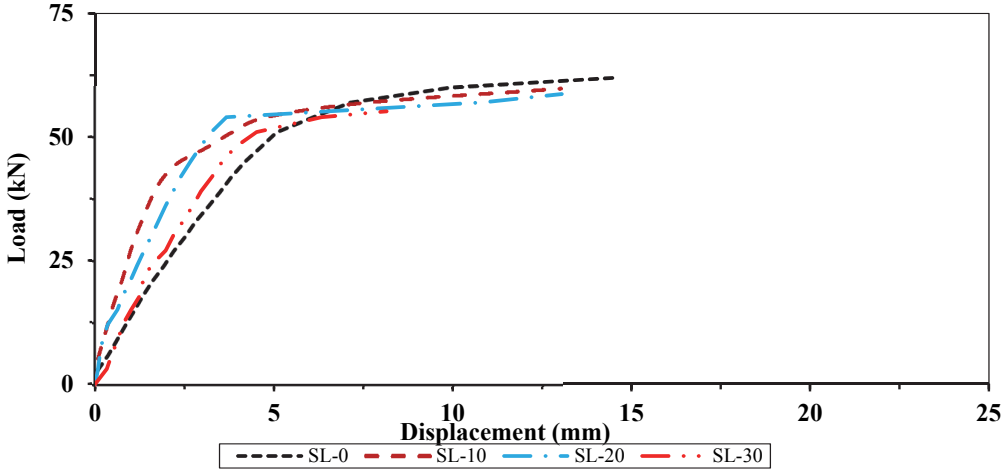

Fig. 6. Load-deflection plots of steel reinforced concrete beams

3.3. Concrete surface strain distribution of steel reinforced beam specimens

The concrete surface strains at mid-span were measured for each load increments using DEMEC points at five positions along the depth of the beam. The measured concrete compressive strains at the top of the beam before initial crack formation were between ranged from 0.013 to 0.031 per cent strain, and before failure, the values varied from 0.22 to 0.36 per cent strain. The highest tensile strain in the beams before initial crack formation was recorded to be 0.11 per cent train, and at ultimate failure, the recorded values ranged from 029 to 0.51 per cent strain. It was observed that beams with up to 10% foam glass content, i.e. SL - 0 and SL - 10 had higher tensile strains before failure compared to beam with foam glass aggregate content greater than 10 per cent, i.e. SL - 20 and SL - 30. The higher strain in beams SL - 0 and SL - 10 may be attributed to higher deflections that were observed for these beams. This also suggests that beams with relatively low foam glass aggregate content had better bond characteristics between steel and the concrete before yielding of the steel. The neutral axis depth was observed to shift upwards towards the compression face due to a marked increase in the tensile strain as the applied load was increased.

3.4 Cracking and mode of failure of BFRP reinforced beam specimens

The reinforcement arrangement for the BFRP RC beams consisted of two 10 mm diameter BFRP bars as tension reinforcement. The first hairline cracks in these beams initiated from the tension face of the beam, under applied loads ranging from 6 to 12 kN, approximately 6 - 25% of their respective ultimate failure loads. Although each beam had a different percentage of foam glass content, the amount of foam

glass in the concrete mix did not have any significant impact on the initial cracking load of the beams. Beyond the first cracking load and during the crack formation phase more secondary hairline flexural cracks were observed at random positions along the tension side of the beams. At approximately 70% of the ultimate failure loads, the cracking in the BFRP beams was stabilised, and no additional cracks were observed. The widths of the cracks that were already formed started to widen with an increase in loads. It also was observed that there were no horizontal cracks at the reinforcement level, which suggests that the concrete and the BFRP rebar had good bond characteristics. Hence bond failure did not occur. All the BFRP reinforced concrete beams consistently failed in compression failure of the concrete as shown in Fig. 7. In particular, the beams failed by concrete crushing before the BFRP bars having developed its full tensile capacity. In this failure mode, the vertical flexural cracks initially developed and extended towards the neutral axis. However, the rate of the crack propagation reduced with the crushing of the concrete at the top compression fibres, the stresses within the top region was therefore redistributed. As the beams were subjected to increased loads, concrete at the top compression fibres started to spall and eventually the beam failed. The concrete crushing failure in the BFRP RC beams may be due to the high ultimate tensile strength of the BFRP bars, which may have caused the deformability of the beams to increase in response to applied loads. Therefore, compression fibres of the concrete reached its maximum strain well before the BFRP bars were able to attain its ultimate strain. As BFRP is a brittle material, structural failure due to BFRP rebar rupture can cause catastrophic consequences. Hence, the over-reinforced design philosophy is generally adopted in structural applications to ensure that a concrete crushing failure occurs before the tensile failure of the BFRP bars.

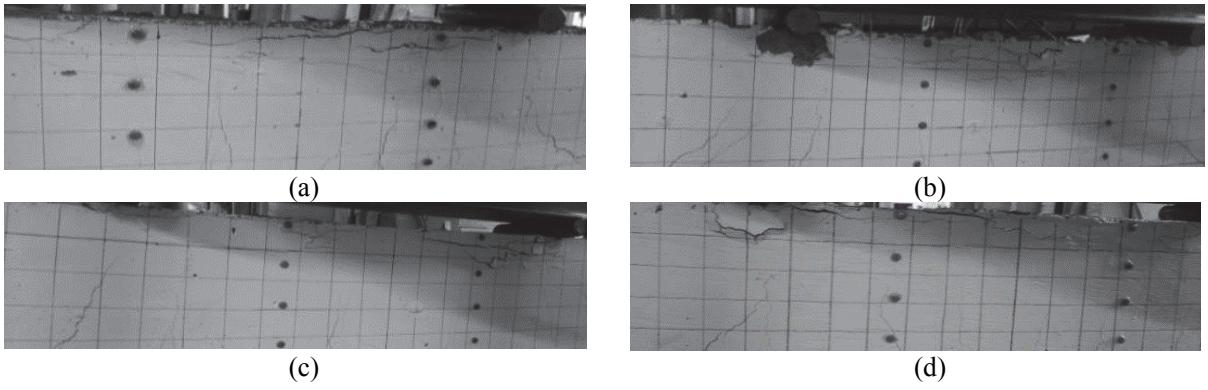

Fig. 7. Failure pattern of BFRP reinforced concrete beams (a) SL-0; (b) SL-10; (c) SL-20; (d) SL-30

3.5 Load-displacement response of BFRP reinforced beam specimens

The mid-span load-deflection relationship of the BFRP reinforced concrete beams is outlined in Fig. 8. The slope of the load-deflection curve shows that the beams generally underwent two distinct stages. During the first stage, represented by the initial linear slope, the beams are un-cracked and are at their elastic stage. Once the first cracks appeared at 6 to 12 kN, a change in the slope the load-deflection curve is observed for all the specimens. Before the cracking load, the beams exhibited similar stiffness. After the first crack, a significant change in the stiffness can be observed for the beams with foam glass content, i.e. beams BF - 1, BF - 2 and BF - 3. The second stage of the load-deflection behaviour (represented by the second slope) is the post-cracking of the concrete. This stage continues until the ultimate failure of the beams occurs. It is apparent that the incorporation of foam glass aggregates has resulted in a decrease in the stiffness of the beams and an increase in the deflection. The deflection of beam BF - 0 at the ultimate failure load of 57 kN was recorded to be 13.6 mm, whereas the deflection for beam BF - 10 before failure load was 20.3 mm. This indicates that 10% of foam glass content resulted in an almost 45% increase in the deflection of the specimen. However, the same behaviour (in terms of increase in deflection) was not observed for specimens BF - 20 and BF - 30, even though these specimens consisted of higher foam glass percentage replacements, the deflections in these two beams were comparable to

BF - 0 which had no foam glass content. This suggests that the addition of foam glass aggregates is more pronounced in decreasing the load capacity rather than a significant role in controlling the deflection.

3.6 Concrete surface strain distribution of BFRP reinforced beam specimens

Similar to the steel reinforced beam specimens, the concrete surface strains were determined. The surface strain recorded at initial crack formation was between 0.000403 and 0.021 per cent strain. However, the readings following the initial crack formation increased remarkably. In the top compression zone of the beams, the maximum strain recorded ranged between 0.11 to 0.54 per cent strain.

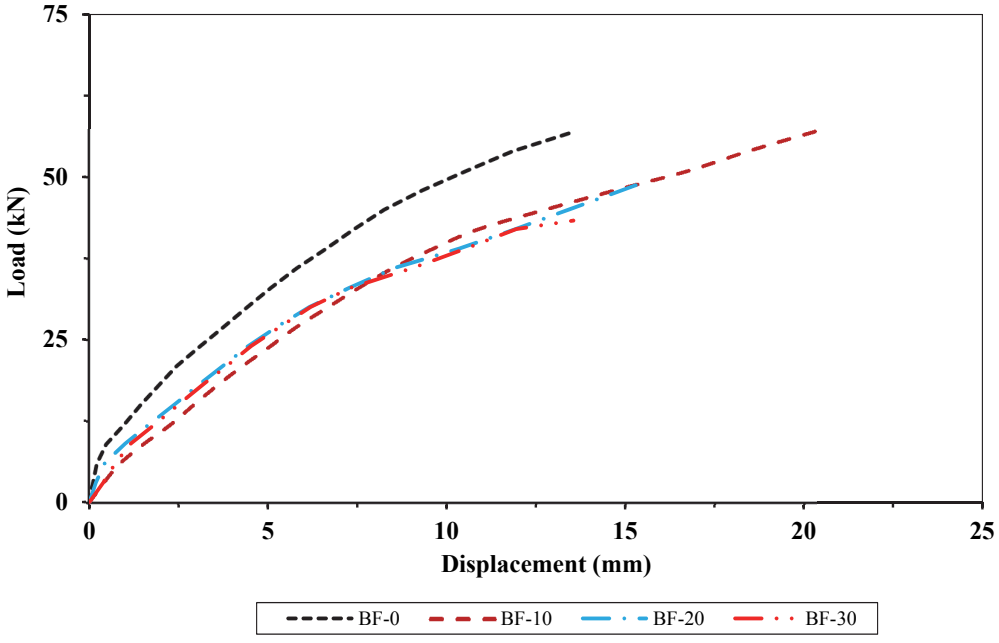

Fig. 8. Load-deflection plots of BFRP reinforced concrete beams

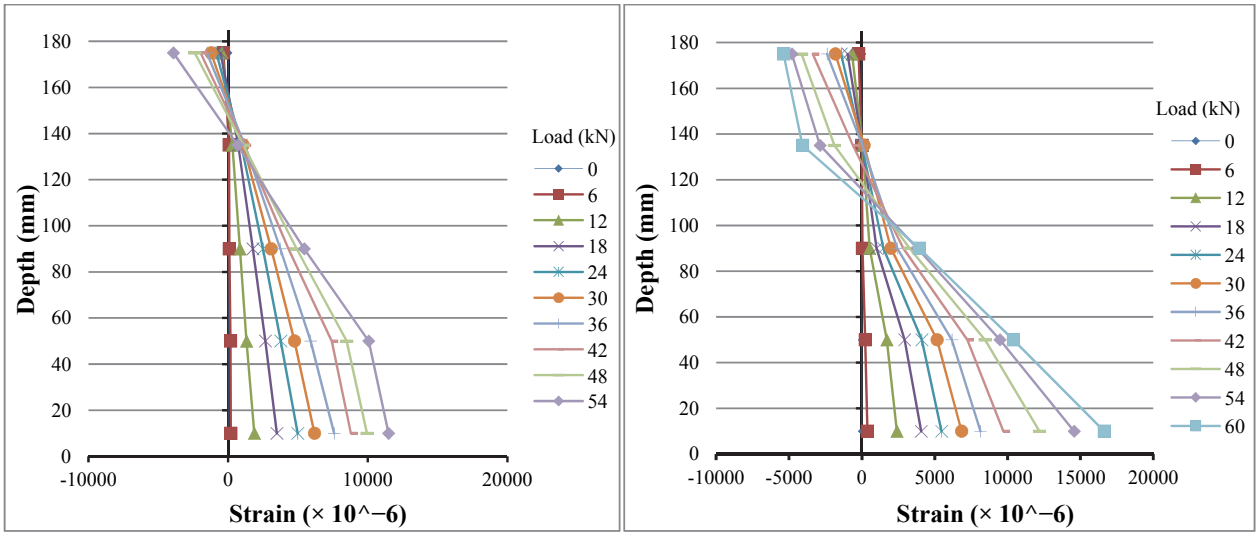

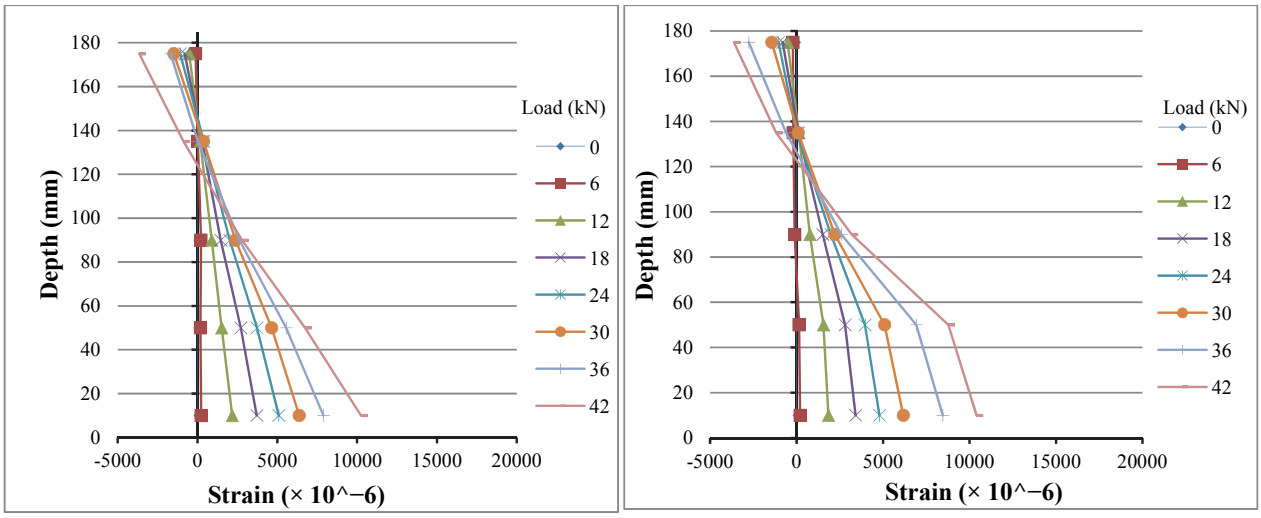

Fig. 9. Strain distributions across depth of BFRP beams (a) BF-0; (b) BF-10; (c) BF-20; (d) BF-30

The maximum tensile strain on the tension side of the concrete surface was determined to be between 0.11 to 1.66 per cent strain. It is worth noting that due to concrete crushing failure, the tensile strain values for all the BFRP reinforced beams did not exceed the yield strain of the BFRP rebar, as expected. The depth of the neutral axis is shown to shift upwards under applied loads, and this continues almost close to the ultimate loading, i.e. 80 to 90% of loading. During the ultimate loading, the neutral axis is shown to shift downwards until the failure of the beam. A possible cause for this downward shift of the neutral axis could be that during the ultimate loading, concrete behaves in a nonlinear manner and with slight stress, more strain is created. However, for BFRP bars the stress-strain relationship is linear. Hence, the downward motion of the neutral axis is necessary for the bending layers to remain flat. The results of this investigation are consistent with the findings of Chitsazan et al. (2010) who reported that, under initial cracking period, the neutral axis of the tested FRP beams shifted upwards and before failure, a downward motion was observed until rupture of the beam. Furthermore, Vijay & GangaRao (2001) found that during the ultimate loading of FRP reinforced concrete beams, a descent of the neutral axis is observed with an increase in loads.

3.7 Load capacities and failure modes

Presented in Table 7 are the loads at first crack formation, and ultimate loads reached for beams tested. The result shows that BFRP beams cracked at an earlier stage in comparison to the equivalent steel reinforced concrete beams. The earliest flexural crack initiation for the BFRP beam series was observed in beam reference BF - 3. The cracking load of the corresponding steel beam, SL - 30 is approximately 40% higher. As the load increased, crack patterns of BFRP reinforced beams were similar to those of the steel equivalent. However, the results indicate that, as the percentage of foam glass content increased, the cracking load decreased by approximately 10 - 40% and approximately 25 - 50% for steel and BFRP reinforced concrete beams, respectively. Also, the spacing of the cracks for both BFRP and steel reinforced concrete beams progressively moved away from the flexural zone. Ovitigala (2012) reported similar observations on a study relating to crack patterns of basalt fibre and steel reinforced concrete beams. The tested beams primarily exhibited two different failure modes. The steel reinforced beams were designed as under reinforced and as such the steel in the tension zone was expected to reach its ultimate limit, at failure, before concrete in the extreme compression fibres reaching its maximum strain of 0.0035 (BS EN 1992) and 0.003 (ACI, 2006). All the steel reinforced beam specimens exhibited typical flexural failure mode by yielding of the steel reinforcement followed by concrete crushing.

Table 7. Flexural test results

Series	Specimen	At first crack		Ultimate		Failure Mode
		Load (kN)	Deflection (mm)	Load (kN)	Deflection (mm)	
Steel	SL-0	21.0	1.61	62.0	14.66	Flexural
	SL-10	19.0	0.71	59.8	13.01	Flexural
	SL-20	16.0	0.77	58.7	13.05	Flexural
	SL-30	15.0	1.00	55.2	8.52	Flexural
BFRP	BF-0	12.0	1.75	57.0	13.56	Concrete crushing
	BF-10	9.0	2.70	57.0	20.29	Concrete crushing
	BF-20	7.0	0.85	48.8	15.33	Concrete crushing
	BF-30	6.0	0.73	43.3	15.55	Concrete crushing

3.8 Code predictions of flexural capacities

The theoretical moment and the ultimate load capacities of the tested beams are compared to the experimental results in this section. Using the balanced FRP reinforcement ratio ρ_{fb} obtained from Eq. (1), the moment capacity (M_u) of the beams with reinforcement ratio ρ_f is greater than ρ_{fb} were predicted using Eq. (2) and Eq. (3) for EC2 and ACI, respectively.

$$\rho_{fb} = 0.85\beta_1 \frac{f'_c}{f_{fu}} \frac{E_f \varepsilon_{cu}}{E_f \varepsilon_{cu} + f_{fu}} \tag{1}$$

$$M_u = \rho_f f_f \left(1 - 0.59 \frac{\rho_f f_f}{f'_c}\right) bd^2 \tag{2}$$

$$M_u = \eta\, 0.85 \frac{f_{ck}}{1.5}\, bd^2 (0.8\, x)\left(1 - \frac{0.8\, x}{2}\right) \tag{3}$$

The ultimate load carrying capacities of the beams tested beams are presented in Table 8, including the values determined from closed form equations in BS EN 1992 and ACI 2006. From the test results, the failure load of specimen BF - 30 is almost 20% less than that of the steel reinforced equivalent, i.e. SL - 30. Similarly, the failure load of steel reinforced beam reference SL - 20 is almost 17% higher than the equivalent BFRP reinforced beam, i.e. BF - 20. Generally, the load capacities of both BFRP and steel reinforced beams are affected by the replacement of foam glass aggregate content. It is evident from the test results that, increasing the percentage content of foam glass aggregate as a proportion of total aggregate weight resulted in decreased load capacity. The reduction is more significant in beams reinforced with BFRP rebars. It seems that the compressive strength of foam glass concrete is a key attribute for the load capacity reduction. Table 8 compares the experimental mid-span moments at failure and the predicted moment capacities derived from Eq. (2) and, Eq. (3). The results show that for beams with steel reinforcements both ACI and EC2 predicted the moment capacities reasonably well in comparison to the experimental results, with an agreement of between 85 - 99.9% for EC2 and 84 - 94% for the ACI code predictions. However, for beams reinforced with BFRP rebars, the moment capacity for beams reference BF - 0, BF - 10, and BF - 30 is underestimated by both EC2 and ACI, i.e. 12.6 - 19% for EC2 and 29 to 30% for ACI, respectively. For the BFRP beam with 20% foam glass aggregate, BF - 20, the prediction is slightly overestimated by EC2 and underestimated by ACI. The statistical mean ratio between the experimental moments and those predicted by EC2 is 0.97, and 0.81 for steel and BFRP reinforced beams, respectively. It is apparent that EC2 derived capacities agree closely with those derived from the ACI equation. The capacity ratio is 1.1, and 0.74 for steel and BFRP reinforced beams, respectively. The ACI moment capacity predictions for the BFRP beams are consistent with the findings of Rafi et al. (2008) who found that the ACI approach underestimated the moment capacity of four tested FRP beams to about 33%. Overall, the beams reinforced with BFRP rebars sustained higher load capacities than capacities derived from ACI and EC2 equations. In the case of the steel reinforced beams, the ACI prediction overestimates all four beams tested, whereas EC2 overestimated beam references SL - 10 and SL - 30 and marginally underestimated beam specimen reference for SL - 20.

Table 8. Comparison of theoretical and experimental load capacities

Series	Specimen	Theoretical prediction				Experimental data			$\frac{P_{theo}}{P_{exp}}$	
		Eurocode 2		ACI						
		M_u (kNm)	P_{theo} (kN)	M_u (kNm)	P_{theo} (kN)	M_{cr} (kNm)	M_u (kNm)	P_{exp} (kN)	$EC2$	ACI
Steel	SL-0	12.5	62.4	13.2	66.0	1.9	12.4	62.0	1.00	0.91
	SL-10	13.0	65.0	13.3	66.5	1.9	12.0	59.8	0.92	0.87
	SL-20	11.3	56.5	13.1	65.5	1.7	11.7	58.7	1.04	1.03
	SL-30	9.3	46.5	12.7	63.5	1.6	11.0	55.2	1.18	1.18
BFRP	BF-0	9.2	45.9	7.8	39.0	1.9	11.4	57.0	1.24	1.46
	BF-10	9.2	45.9	8.1	40.5	1.9	11.4	57.0	1.24	1.41
	BF-20	8.6	43.0	7.0	35.0	1.7	8.0	48.8	1.13	1.39
	BF-30	7.6	38.0	6.1	38.0	1.6	8.7	43.3	1.14	1.13

4. Concluding remarks

The experimental results describing the flexural behaviour of eight lightweight reinforced concrete beams are presented herein. Four basalt FRP reinforced concrete beams, and four high yield steel reinforced concrete beams have been tested for flexure under four-point loading arrangement. The measured deflections, crack propagations, experimental moments, mode of failure and ultimate load carrying capacity for both series of beams have been analysed and compared between them. Also, theoretical models proposed by BS EN 1992 – Eurocode 2 and ACI for the prediction of deflections and flexural capacities for both steel and basalt FRP reinforced concrete beams were also compared. Within the scope of the experimental and analytical findings reported in this paper, the most relevant concluding remarks can be summarised as follows:

1) The behaviour of both steel and BFRP reinforced beams were linear until the first crack occurred. However, due to lack of plasticity in the BFRP bars, beams reinforced with BFRP continued to exhibit linear behaviour until failure.
2) Deflections for beams with BFRP reinforcement were significantly higher in comparison to steel reinforced beams, due to the much lower modulus of BFRP reinforcement.
3) Corresponding to the design characteristics, the mode of failure in BFRP beams was predominantly concrete crushing.
4) The cracking load for BFRP reinforced beams were up to 40% higher in comparison to similar beams reinforced with steel.
5) The increase in foam glass aggregate content was observed to reduce the cracking load by almost 10 - 40% and 25 - 50% for steel and BFRP reinforced concrete beams, respectively.
6) The load carrying capacity of BFRP reinforced beams were almost 20% lower than their comparable steel reinforced beams. Furthermore, the load capacities of both BFRP and steel reinforced beams are decreased with an increase in foam glass content.
7) The theoretical flexural capacities of BFRP reinforced beams were underestimated by both ACI 440.1R (2006) and Eurocode 2 prediction models.

Acknowledgement

The authors are particularly thankful to the technicians, Mr Kieran Teeling and Mr Ian Breakwell of the School of Energy, Construction and Environment, Coventry University, for their assistance in the fabrication of test specimens. The authors also gratefully acknowledge the support of MagmaTech Ltd., UK, supplier of the BFRP rebar.

References

ACI Committee 440. (2003). Guide for the design and construction of concrete reinforced with FRP bars. ACI 440.1R-03, Detroit, USA.

ACI Committee 440. (2006). ACI 440.1R-06. Guide for the design and construction of concrete reinforced with FRP bars. American Concrete Institute (ACI), Farmington Hills, Michigan, USA.

Aliha, M. R. M., Heidari-Rarani, M., Shokrieh, M. M., & Ayatollahi, M. R. (2012). Experimental determination of tensile strength and K (IC) of polymer concretes using semi-circular bend(SCB) specimens. *Structural Engineering and Mechanics*, *43*(6), 823-833.

Aliha, M. R. M., Razmi, A., & Mansourian, A. (2017). The influence of natural and synthetic fibers on low temperature mixed mode I+ II fracture behavior of warm mix asphalt (WMA) materials. *Engineering Fracture Mechanics*, *182*, 322-336.

Aliha, M. R. M., Razmi, A., & Mousavi, A. (2018). Fracture study of concrete composites with synthetic fibers additive under modes I and III using ENDB specimen. *Construction and Building Materials*, *190*, 612-622.

Alnahhal, W., & Aljidda, O. (2018). Flexural behavior of basalt fiber reinforced concrete beams with recycled concrete coarse aggregates. *Construction and Building Materials*, *169*, 165-178.

Alsayed, S. H., Al-Salloum, Y. A., & Almusallam, T. H. (2000). Performance of glass fiber reinforced plastic bars as a reinforcing material for concrete structures. *Composites Part B: Engineering*, *31*(6-7), 555-567.

Ashour, A. F., & Habeeb, M. N. (2008). Continuous concrete beams reinforced with CFRP bars. Proceedings of the Institution of Civil Engineers. 161 (6), 349-357.

Awang, H., Ahmad, M. H., & Al-Mulali, M. Z. (2015). Influence of kenaf and polypropylene fibres on mechanical and durability properties of fibre reinforced lightweight foamed concrete. *Journal of Engineering Science and Technology*, *10*(4), 496-508.

Bakis, C. E., Bank, L. C., Brown, V., Cosenza, E., Davalos, J. F., Lesko, J. J., ... & Triantafillou, T. C. (2002). Fiber-reinforced polymer composites for construction—State-of-the-art review. *Journal of composites for construction*, *6*(2), 73-87.

Barris, C., Torres, L., Miàs, C., & Vilanova, I. (2012). Design of FRP reinforced concrete beams for serviceability requirements. *Journal of Civil Engineering and Management*, *18*(6), 843-857.

Benmokrane, B., & Masmoudi, R. (1996). Flexural response of concrete beams reinforced with FRP reinforcing bars. *Structural Journal*, *93*(1), 46-55.

Benmokrane, B., Chaallal, O., & Masmoudi, R. (1995). Glass fibre reinforced plastic (GFRP) rebars for concrete structures. *Construction and Building Materials*, *9*(6), 353-364.

Brady, K. C., Jones, M. R., & Watts, G. R. (2001). *Specification for foamed concrete*. TRL Limited.

Brik, V. (2003). Advanced concept concrete using basalt fiber/BF composite rebar reinforcement. *IDEA Project*, *86*, 71-71.

BS EN 1992-1-1 (2004). Eurocode 2: Design on Concrete Structures – Part 1-1: General Rules and Rules for Building. London: British Standards Institution.

Chitsazan, I., Kobraei, M., Zamin, M. J., & Shafigh, P. (2010). An experimental study on the flexural behaviour of FRP RC beams and a comparison of the ultimate moment capacity with ACI. Journal of Civil Engineering and Construction Technology. 1 (2), 27-42.

Cosenza, E., Manfredi, G., & Realfonzo, R. (1997). Behavior and modeling of bond of FRP rebars to concrete. *Journal of composites for construction*, *1*(2), 40-51.

El-Salakawy, E. F., Polak, M. A., & Soudki, K. A. (2002). Rehabilitation of reinforced concrete slab column connections. *Canadian Journal of Civil Engineering*, *29*(4), 602-611.

El-Sayed, A. K., El-Salakawy, E. F., & Benmokrane, B. (2006a). Shear capacity of high-strength concrete beams reinforced with FRP bars. *ACI Structural Journal*, *103*(3), 383.

El-Sayed, A. K., El-Salakawy, E. F., & Benmokrane, B. (2006b). Shear strength of FRP-reinforced concrete beams without transverse reinforcement. *ACI Structural Journal*, *103*(2), 235.

Fakhri, M., Amoosoltani, E., & Aliha, M. R. M. (2017). Crack behavior analysis of roller compacted concrete mixtures containing reclaimed asphalt pavement and crumb rubber. *Engineering Fracture Mechanics*, *180*, 43-59.

Faza, S. S., & Gangarao, H. V. (1993). Theoretical and experimental correlation of behavior of concrete beams reinforced with fiber reinforced plastic rebars. *Special Publication*, *138*, 599-614.

GangaRao, H. V. S., & Vijay, P. V. (1997, October). Design of concrete members reinforced with GFRP bars. In *Proc., 3rd Int. Symposium, Fiber Reinforced Polymer Reinforcement for Reinforced Concrete Structures* (Vol. 1, pp. 143-150).

Gao, D., Benmokrane, B., & Masmoudi, R. (1998). *A calculating method for flexural properties of FRP-reinforced concrete beam*. Department of Civil Engineering, Faculty of Engineering, University of Sherbrooke.

Gohnert, M, Van Gool, R & Benjamin, M. (2014). Basalt reinforcement in concrete beams. The Structural Engineer. 93 (1), p38-43.

Hassoun, M. N., & Al-Manaseer, A. (2012). *Structural concrete: theory and design*. John wiley & sons.

Heidari-Rarani, M., Aliha, M. R. M., Shokrieh, M. M., & Ayatollahi, M. R. (2014). Mechanical durability of an optimized polymer concrete under various thermal cyclic loadings–An experimental study. *Construction and Building Materials*, *64*, 308-315.

Hollaway, L. C. (2010). A review of the present and future utilisation of FRP composites in the civil infrastructure with reference to their important in-service properties. *Construction and building materials*, *24*(12), 2419-2445.

Jones, M. R., & McCarthy, A. (2005). Preliminary views on the potential of foamed concrete as a structural material. *Magazine of concrete research*, *57*(1), 21-31.

Kara, I. F., & Ashour, A. F. (2012). Flexural performance of FRP reinforced concrete beams. *Composite structures*, *94*(5), 1616-1625.

Khatib, J. M., Shariff, S., & Negim, E. M. (2012). Effect of incorporating foamed glass on the flexural behaviour of reinforced concrete beams. *World Applied Sciences Journal*, *19*(1), 47-51.

Kılıç, A., Atiş, C. D., Yaşar, E., & Özcan, F. (2003). High-strength lightweight concrete made with scoria aggregate containing mineral admixtures. *Cement and Concrete Research*, *33*(10), 1595-1599.

Limbachiya, M., Meddah, M. S., & Fotiadou, S. (2012). Performance of granulated foam glass concrete. *Construction and building materials*, *28*(1), 759-768.

Mansourian, A., Hashemi, S., & Aliha, M. R. M. (2018). Evaluation of pure and mixed modes (I/III) fracture toughness of Portland cement concrete mixtures containing reclaimed asphalt pavement. *Construction and Building Materials*, *178*, 10-18.

Mostofinejad, D., & Moghaddas, A. (2014). Bond efficiency of EBR and EBROG methods in different flexural failure mechanisms of FRP strengthened RC beams. *Construction and Building Materials*, *54*, 605-614.

Nanni, A. (1993). Flexural behavior and design of RC members using FRP reinforcement. *Journal of structural engineering*, *119*(11), 3344-3359.

Nanni, A. (2003). North American design guidelines for concrete reinforcement and strengthening using FRP: principles, applications and unresolved issues. *Construction and Building Materials*, *17*(6-7), 439-446.

Ovitigala, T. (2012). Structural behaviour of concrete beams reinforced with basalt fibre reinforced polymer (BFRP) bars. PhD thesis, Univ. of Illinois, Chicago.

Rafi, M. M., Nadjai, A., Ali, F., & Talamona, D. (2008). Aspects of the behaviour of CFRP reinforced concrete beams in bending. Construction and Building Materials 22 (3), 277-285.

Razmi, A., & Mirsayar, M. M. (2017). On the mixed mode I/II fracture properties of jute fiber-reinforced concrete. *Construction and Building Materials*, *148*, 512-520.

Rooholamini, H., Hassani, A., & Aliha, M. R. M. (2018a). Evaluating the effect of macro-synthetic fibre on the mechanical properties of roller-compacted concrete pavement using response surface methodology. *Construction and Building Materials*, *159*, 517-529.

Rooholamini, H., Hassani, A., & Aliha, M. R. M. (2018b). Fracture properties of hybrid fibre-reinforced roller-compacted concrete in mode I with consideration of possible kinked crack. *Construction and Building Materials*, *187*, 248-256.

Sæther, I. V. (2010). Structural behaviour of deteriorated and retrofitted concrete structures.

Song, H. W., & Saraswathy, V. (2007). Corrosion monitoring of reinforced concrete structures-A. *Int. J. Electrochem. Sci*, *2*, 1-28.

Tureyen, A. K., & Frosch, R. J. (2002). Shear tests of FRP-reinforced concrete beams without stirrups. *Structural Journal*, *99*(4), 427-434.

Urbanski, M., Lapkob, A., & Garbacz, A. (2013). Investigation on Concrete Beams Reinforced with Basalt Rebars as an Effective Alternative of Conventional R/C Structures. Procedia Engineering (57), 1183 – 1191.

Vijay, P. V., & GangaRao, H. V. S. (2001). Bending behaviour and deformability of glass fibre-reinforced polymer reinforced concrete members. ACI Struct J, 98 (6) (2001), pp. 834-842.

Wang, H., & Belarbi, A. (2005). Flexural behavior of fiber-reinforced-concrete beams reinforced with FRP rebars. *ACI Structural Journal, SP230*, *51*(230), 895-914.

West, J. S. (2011). An Introduction to FRP-Reinforced Concrete. ISIS Canada Educational Module No. 3: An Introduction to FRP-Reinforced Concrete (2), 1-60.